POLITECNICO
MILANO 1863

SCUOLA DI INGEGNERIA INDUSTRIALE
E DELL'INFORMAZIONE

EXECUTIVE SUMMARY OF THE THESIS

Design and Validation of Planar Setups for the Characterization of TRISTAN Detectors

TESI MAGISTRALE IN ELECTRONICS ENGINEERING – INGEGNERIA ELETTRONICA

AUTHOR: ALESSIO PIGLIAFREDDO

ADVISOR: PROF. MARCO CARMINATI

CO-ADVISOR: DR. MATTEO GUGIATTI

ACADEMIC YEAR: 2021-2022

1. Introduction

Dark matter is a hypothetical form of matter present in the universe whose origin have been proposed by different theories. Since the dark matter almost does not interact with normal matter and electromagnetic radiation, but only through gravitational forces, a promising candidate, who can account for at least a part of the missing mass, is the neutrino. Indeed, this subatomic particle does not interact with the strong nuclear force and is only weakly affected by the gravitational force and the weak nuclear force. Up to now the neutrino is the only particle of the Standard Model which was observed exclusively with left-handed chirality, due to its interaction with the weak nuclear force. The presence of another type of neutrino, with right-handed chirality, has been hypothesised but not experimentally confirmed yet [1]. In opposition to left-handed neutrinos, which are called "active", these right-handed neutrinos are called "sterile", since they interact just via gravity and not through any of the Standard Model's fundamental interactions. The active neutrinos have a too small mass to account for all the dark matter, whereas sterile neutrinos are predicted to be significantly heavier, and so they may have a key role in the dark matter.

1.1. KATRIN experiment

The KATRIN (KArlsruhe TRItium Neutrino) experiment, at the Karlsruhe Institute of Technology (KIT), is trying to determine the electron antineutrino mass (m_{ν_e}) by searching for a shift of the endpoint (18.6 keV) of the tritium β^- decay spectrum (Figure 1.1).

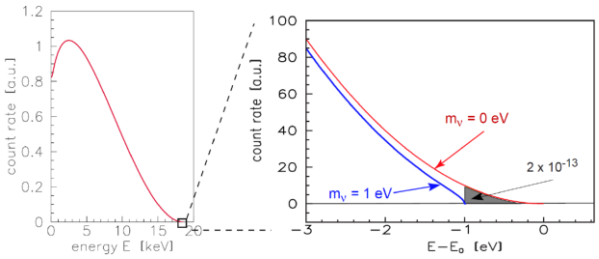

Figure 1.1: *Tritium β^- spectrum endpoint region with $m_{\nu_e} = 0$ eV/c² (red line) and $m_{\nu_e} = 1$ eV/c² (blue line).*

Indeed, tritium decays into ^{3}He emitting an electron and an electron antineutrino. The rest masses of electron and antineutrino are constant, while the remaining energy is divided between the two particles kinetic energy based on a given statistics. So, by measuring the electrons kinetic energy, focusing on the region near to the β^- decay endpoint energy E_0, it is possible to derive the antineutrino mass. To do such a measurement, in the KATRIN experimental setup, a MAC-E spectrometer acts as a high pass energy filter for the electrons generated by the tritium source. This allows to set a given threshold so that electrons with insufficient kinetic energy are reflected back, while those with enough energy can pass and be measured by a 148-pixel pin-diode detector. These measurements resulted in the determination of an upper limit neutrino mass of 1.1 eV.

1.2. TRISTAN experiment

The TRISTAN project (TRitium Investigation on STerile to Active Neutrino mixing) is an extension of the KATRIN physics program. The plan is to make use of the KATRIN spectrometer and its beamline to search for the signature of sterile neutrinos with masses in the keV range by measuring the entire tritium β^- decay spectrum [2]. Looking at this spectrum in fact: the active neutrinos produce a distortion close to the endpoint energy E_0; the superposition of this hypothetical sterile neutrino instead would result in the presence of a kink at $E_{kink} = E_0 - m_s$, with m_s being the sterile neutrino mass, as shown in Figure 1.2. The distance of the "kink like" signature from E_0 is equal to the mass of the sterile neutrino.

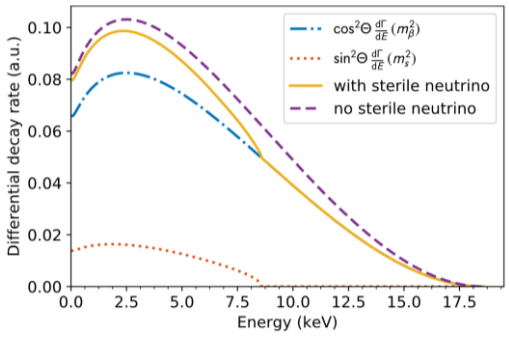

Figure 1.2: *Entire tritium β^- decay spectrum in case of $m_s = 10$ keV and $\sin^2(\vartheta) = 0.2$. The blue and orange lines represent respectively the decay branch into a light active neutrino and into a sterile neutrino. The solid yellow line is given by the superposition of the two previous lines, showing the kink-like distortion. The purple line represents the case without sterile neutrino.*

Differently from the KATRIN experiment, to search for the keV-scale sterile neutrinos the spectrum measurement interval must be extended to cover the entire energy range. This requires to decrease the spectrometer energy threshold. In this way, the number of electrons driven to the detector will be several orders of magnitude higher and the actual detector, based on pin diodes, is not able of handling such a high count rate. This is the reason why TRISTAN requires a new detector, based on 21 modules of 166-pixel monolithic SDDs each, for a total of 3486 pixels, capable of detecting very tiny spectrum distortions and handling a total rate up to 10^8 cps, that will be integrated into KATRIN setup. Following a "step-by-step approach", different sizes of SDD matrices have been produced and tested, and the main prototypes are the 12-, 47- and 166-pixel versions.

To readout the TRISTAN detector pixels, a custom ASIC, called ETTORE [3], has been used. It is a 12-channel ASIC, each of which features a first stage Charge Sensitive pre-Amplifier (CSA), a second AC-coupled amplification stage and a comparator. The latter is used to inform the reset logic of the saturation of the CSA output, which is the superposition of a ramp-like signal, due to the integration of leakage current on the feedback capacitance (C_F), and step-like signals corresponding to the detected events. The external electronics will then reset the charge integrated on C_F by imposing a given voltage drop across it. Alternatively, it is possible to provide a periodic reset. As mentioned, each ASIC can readout 12 pixels, so the larger detector versions are built by multiple replicas of this 12-pixel elementary structure and readout by more than one ETTORE thanks to dedicated ASIC boards hosting the chips. Figure 1.3 illustrates the acquisition chain for the readout of the 166-pixel detector. The SDD is coupled to ETTORE and read by a data acquisition system composed of a bias board, to supply both the ASICs and the detector and to buffer the ASIC outputs, and a Digital Acquisition (DAQ) system, called Athena, to digitalize the output signals.

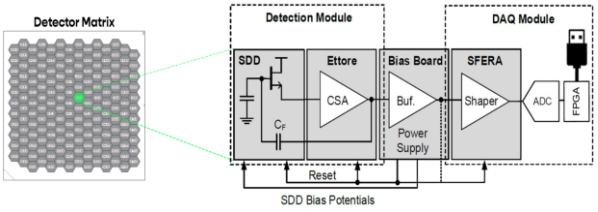

Figure 1.3: *Electronic acquisition chain.*

2. 166-pixel Bias System

During the development of the TRISTAN project, to move from the 47-pixel to the 166-pixel planar setup, it was required a new bias system, able to provide the supply to the 166-pixel detector and the two 83-channels ASIC boards attached to it, to manage the ASIC control signals and the SDD reset and to interconnect the 166 ASIC boards outputs with the DAQ inputs. A commercial bias system was under development by an external company (XGLab S.r.l.) and will be employed for the installation inside the spectrometer. For the laboratory setup instead, a more compact system was required to perform the preliminary 166-pixel detector characterizations. Thus, in the bias system developed in this thesis, called Lifeboard, the buffer stage was not implemented, since it was not essential due to the short interconnections in the laboratory setup. The voltage and current requirements of the 166-pixel setup, that this bias system has to satisfy, are shown in Figure 2.1. It also specifies if the voltages have fixed values (*fixed*) or can be adjusted with trimmers (*adj.*) and if it is sent independently to the two ASIC boards (*hemisphere*) or sent in parallel to both (*global*).

Feature	Voltage	Max. current	Type
ASIC board supply (V_{IO})	4.1 V	700 mA	Fixed, hemisphere
ASIC ref. (V_{REF}, V_{TH}, V_{BW})	0÷3.3 V	1 mA	Adj. global
JFET drain (V_D)	1.22÷13.42 V	50 mA	Adj. global
JFET bias generator (V_{SSS})	-1.22÷-13.42 V	-50 mA	Adj. hemisphere
SDD reset diode high (V_{RES_H})	0÷10 V	200 µA	Adj. hemisphere
SDD reset diode low (V_{RES_L})	0÷-15 V	-200 µA	Adj. hemisphere
SDD inner guard ring (V_{IGR})	0÷-26.3 V	-10 µA	Adj. global
SDD first ring (V_{R1})	-1.58÷-13.78 V	10 mA	Adj. global
SDD last ring (V_{RX})	-95÷-145 V	-10 mA	Adj. global
SDD back frame (V_{BF})	0÷-150 V	-10 µA	Adj. global
SDD back contact (V_{BC})	0÷-150 V	-10 µA	Adj. global

Figure 2.1: *List of bias voltages and currents in the Lifeboard bias system.*

The Lifeboard is composed by three boards: a main bias board and two identical 83-channel connection boards placed over it, as illustrated in Figure 2.2. The bias board generates the bias voltages and the control signals both for the SDD matrix and for ETTORE ASICs. Instead, the purpose of the connection boards is to send the ETTORE outputs to the DAQ.

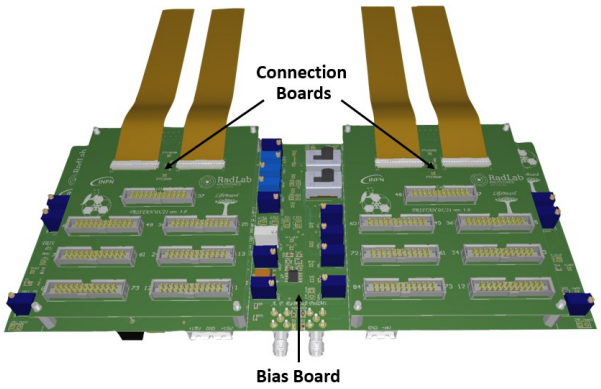

Figure 2.2: *3D CAD model of the Lifeboard.*

2.1. Bias Board

The bias board is divided in different sections. The **positive and negative low voltages section,** which takes the ±15 V supply from an external voltage generator and, through a DC-DC converter and some LDO regulators, provides the ASIC board supply (V_{IO}), the JFET drain voltage (V_D), the JFET bias generator voltage (V_{SSS}) and the ASIC reference voltage (V_{ASIC}) that is used to generate the reference signals for the ASICs. The **reference voltages section**, that provides the V_{REF}, the V_{TH}, the V_{BW} and the *select_pre* signal (use to select either the first stage or the second stage ETTORE output to be sent to the output lines). The **reset section**, driven by an external reset (*RES_EXT*) taken from an external pulse generator by an SMA connector. The *RES_EXT* is used to drive the circuits that provide the reset signal to the SDDs and the inhibit signal to the ASICs. The **detector bias section**, supplied by an external high voltage generator (-150 V) and providing, through trimmers and LDO regulators, both the high voltages (V_{BC}, V_{BF} and V_{RX}) and the inner guard ring voltage (V_{IGR}) for the detector. The first ring voltage is instead set independently and supplied by the ±15 V voltage generator. This section features a diode protection mechanism to prevent damages when switching off the V_{IGR} without having completely discharged the V_{BC}, V_{BF} and V_{RX} voltages. The **interconnection section**, featuring two 40-pin board-to-board connectors to provide the signals and the bias voltages to the connection boards.

2.2. Connection Board

The connection board features seven 24-pin connectors to the DAQ, two test points to measure the voltage across the PT1000 sensor present in the

ASIC board, two 100-pin connectors to connect the connection board to the ASIC board through two dual-layer flexible printed circuits (FPC) cables and the 40-pin board-to-board connector to connect the connection board to the bias board.

3. In air 166-pixel module characterization

3.1. Preliminary characterization

The Lifeboard bias system allowed to perform the first 166-pixel detector characterization. The operation of a monolithic SDD detector of this size represents a relevant milestone in this field. The spectroscopy characterization measurements were performed using a ^{55}Fe radioactive source and a shaping time of 6 μs. The SDD detector was cooled down to 0 °C and the acquisition lasted 300 s. Figure 3.1 shows the 166 calibrated spectra acquired with the setup. In most of them the Mn-Kα and Mn-Kβ lines are well visible, while some pixels present distortions in the spectrum shape, caused either by charge loss mechanisms in the device or by random telegraphic signals (RTS). Due to contaminations during the fabrication process, the detector has an unexpected not negligible drain line resistance that made critical the correct biasing of all the pixels simultaneously.

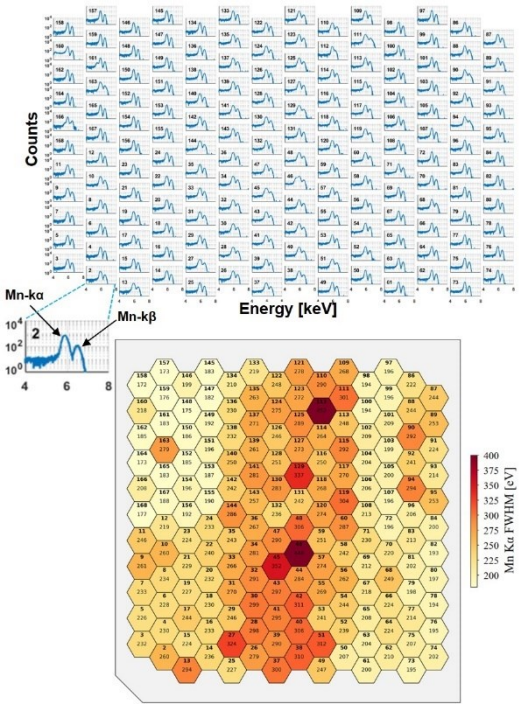

Figure 3.1: *166 pixels calibrated ^{55}Fe spectra (top) and energy resolution (FWHM) at the Mn-kα line (bottom).*

Therefore, in the setting of the bias voltages, a compromise has been made trying to minimize the pixels affected by spectrum distortions. In the bottom side of the figure, the FWHM at the 5.898 keV Mn-kα line of each pixel is shown. On average the resolution is quite good and can be further enhanced by cooling the detector below 0 °C. Finally, to test the homogeneity of the matrix, the event rate of each pixel and the gain of each channel were measured. Their results showed an extremely uniform behaviour.

3.2. Stability measurement

Another important parameter of the system is the stability over a long time measurement. The system performances measured before, with 300 s measurements, may vary over time and with temperature variations giving different results every time a test is performed. Therefore, a long time (53 h) measurement, monitoring the temperature of the DAQ (specifically of Kerberos APP boards [4]) and of the ASIC board, is required to have a clearer understanding of the system behaviour. The monitoring of the temperature was done by designing a simple amplifying circuit to readout two PT1000 sensors and by using the data logger functionality of the Moku:Go tool [5]. The results of this measurement are reported in Figure 3.2. The FWHM appears almost independent on the temperature up to about T_{ASIC} = 33 °C or $T_{Kerberos}$ = 27 °C. After these values it shows a small increase, but only few measurements were acquired in this region, so there are too small statistics.

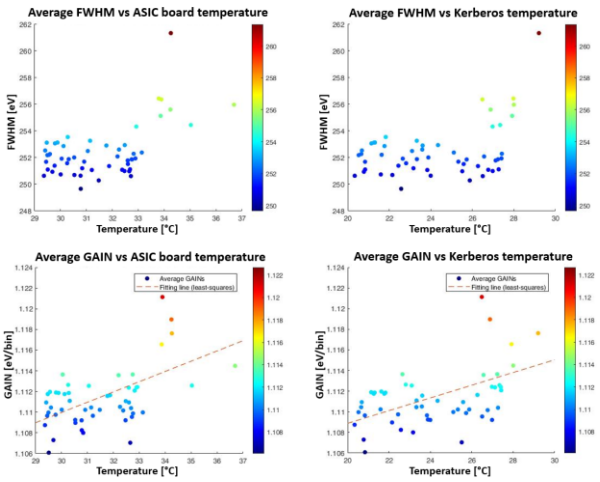

Figure 3.2: *Average FWHM vs ASIC board or Kerberos temperature (top plots); average GAIN vs ASIC board or Kerberos temperature (bottom plots).*

The GAIN instead slightly increases with temperature and, fitting the scatter plot with a line that minimizes the square distances, it is possible to compute a gain increase of 9.9×10^{-4} eV/bin for each degree of temperature increase of the ASIC board, while, if Kerberos temperature increases by one degree, the gain increases of 6.1×10^{-4} eV/bin.

4. In vacuum 47-pixel module

The detector response to electrons is much different and more complex than the response to X-ray photons. This originates from the incomplete charge collection happening in the partially sensitive entrance window region of the detector and from the fact that electrons can backscatter. Since in TRISTAN experiment the detectors are hit by electrons generated from the tritium β- decay, a deep understanding and modelling of the detector response was needed. To be able to test the SDD detectors with different sources (X-rays, electrons, …) and using ancillary detectors to collect more information (e.g. backscattering), a testing vacuum setup was needed.
To study the detector response to electrons accelerated with different energies, a photoelectric based electron gun has been implemented (Figure 4.1). The SDD detector is placed underneath the anode plate of the electron gun and the electrons can impinge on it thanks to a little hole (1 mm) made on the plate and acting as a collimator.

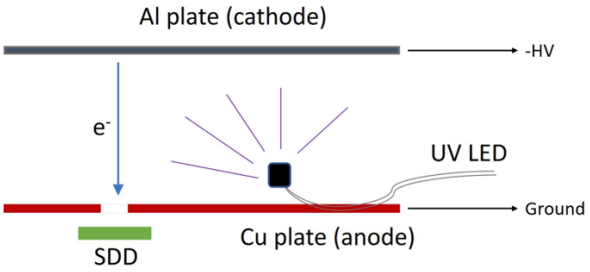

Figure 4.1: *Photoelectric based electron gun structure.*

4.1. 12-pixel setup

An existing vacuum setup, for the characterization of the 12-pixel detector with the electron gun, was already present in the Department of Physics of Milano-Bicocca University. The vacuum environment is provided by a vacuum chamber featuring a sophisticated cooling system based on liquid nitrogen or chilled fluid. A CF100 flange, hosting four 27-pin Fischer connectors, is used to bring all the electrical signals inside the chamber. The electron gun can be moved along X and Y axis by a manually regulated mechanical movement system. This is useful to perform charge sharing measurements by moving the electron gun across the pixel matrix. The vacuum setup can perform backscattering measurements by using a ^{109}Cd radioactive source hitting a passive (block of Si) or active (single pixel detector) target and measuring the backscattered electrons with the 12-pixel detector.

4.2. 47-pixel setup

To move from the 12-pixel to the 47-pixel vacuum setup, a new vacuum-air interconnection system was required. The vacuum chamber structure was already compatible with the 47-pixel module, so no changes have been introduced, whereas the CF100 flange has been completely redesigned to account for the larger number of output channels present on the 47-ch ASIC board. The new flange (Figure 4.2) hosts six 27-pin Fischer connectors: one of them is used to provide the control and biasing voltages to the detector and the ASIC board; four connectors are employed to brings the ASICs outputs outside the chamber; one is used to bias the UV LED and a new vacuum compatible stepper motor movement system used to automatically move the electron gun. This last connector is directly linked with the LED and the movement system, whereas the other connectors must be adapted to the two 100-pin connectors present on the ASIC board.

Figure 4.2: *3D model of the flange (left). Picture of the six 27-pin connectors mounted on the flange (right).*

For this reason, it has been designed an interconnection board, called *Luna board*, which has been placed on top of the flange, soldered to the connectors, as shown in Figure 4.3. The Fischer connectors pads are placed at five vertices of a hexagon, following the flange geometry, while the

100-pin connectors are placed in the central region allowing to have enough space to attach the FPC cables without too sharp angles which may cause damages or even break the cables.

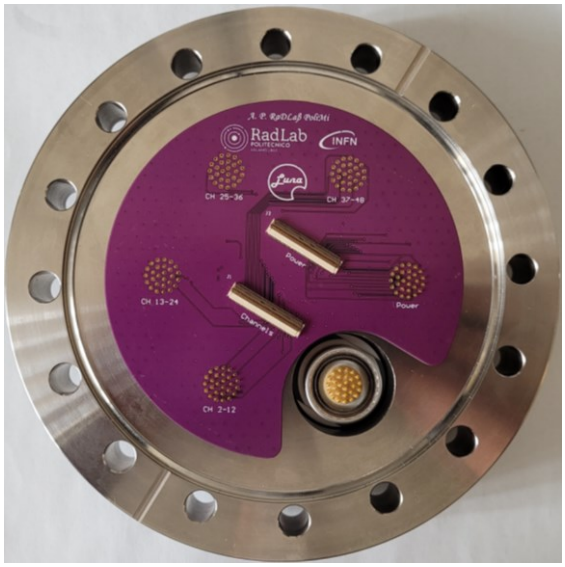

Figure 4.3: *Vacuum-air interconnection system for the 47-pixel vacuum setup.*

5. Conclusions

The first bias system for the new 166-pixel TRISTAN module was developed during this thesis, allowing to perform the preliminary in-air characterization of the novel 166-pixel SDD detector, which is a relevant milestone in this field, and to test the 83-channel ASIC boards. The spectroscopy measurements, performed using a ^{55}Fe radioactive source, showed a quite good energy resolution, not optimal due to an unexpected larger drain line resistance, and a good matrix homogeneity. In the next months, the 166-pixel detectors of a new wafer production, implementing design modifications to mitigate the resistance issue, are going to be tested and then mounted in the 3D 166-pixel module (Figure 5.1).
The stability of the 166-pixel planar system was tested by doing a long time measurement monitoring both the performance variations over time and the variations over temperature. The temperature monitoring was done by designing a simple amplifying circuit to readout two PT1000 sensors and using a data logger. This measurement discovered a small increase of the channel gain with temperature and a not clear dependence of the FWHM with temperature. Overall, the stability is good and the small gain variation is tolerable.

The final part of this thesis concerned the development of a new vacuum-air interconnection system to move from the 12-pixel vacuum setup to the 47-pixel one. This vacuum setup is important to study and model the SDD detector response to electrons, here generated and accelerated by an electron gun, and to analyse the backscattering phenomena. Understanding these interactions is fundamental since, in the final TRISTAN experiment, the detectors will be hit by electrons generated from the tritium β^- decay.

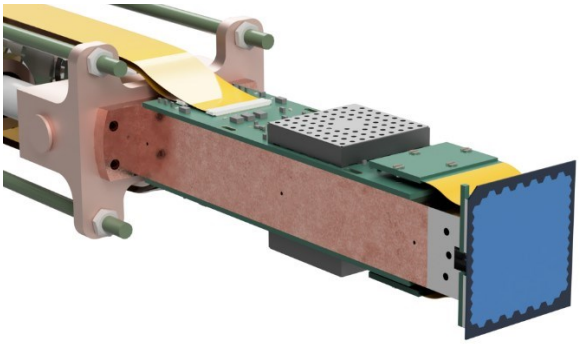

Figure 5.1: *3D 166-pixel module.*

References

[1] L. Canetti, M. Drewes, and M. Shaposhnikov, “Sterile neutrinos as the origin of dark and baryonic matter”, Physical review letters, vol. 110, no. 6, p. 061 801, 2013.

[2] S. Mertens et al. *A novel detector system for KATRIN to search for keV-scale sterile neutrinos. Journal of Physics G: Nuclear and Particle Physics*, 46(6):065203, 2019.

[3] P. Trigilio, L. Bombelli, M. Carminati, R. Bisognin, A. Grande, M. Gugiatti, C. Fiorini, P. Lechner, T. Brunst, and S. Mertens, *ETTORE: a 12-Channel Front-End ASIC for SDDs with Integrated JFET, in 2018 IEEE Nuclear Science Symposium and Medical Imaging Conference Proceedings (NSS/MIC), IEEE*, 2018, pp. 1–4.

[4] P. King, G. Torrisi, M. Gugiatti, M. Carminati, S. Mertens, and C. Fiorini. *Kerberos: a 48-Channel Analog Processing Platform for Scalable Readout of Large SDD Arrays. In 2019 IEEE Nuclear Science Symposium and Medical Imaging Conference (NSS/MIC)*, pages 1–3, 2019.

[5] ‘Moku:Go’, Liquid Instruments. https://www.liquidinstruments.com/products/hardware-platforms/mokugo/ (accessed Mar. 15, 2022).